Integral-Optimal Sliding Mode Control for Vertical Take-Off and Landing System

Xavier Aguas, Jefferson Revelo, Israel Paredes, Andrés Cuaycal, Marco Herrera
Departamento de Automatización y Control Industrial
Escuela Politécnica Nacional
Quito, Ecuador
{xavier.aguas, jefferson.revelo, israel.paredes, andres.cuaycal, marco.herrera}@epn.edu.ec

***Abstract*—In this paper an Integral Sliding Mode Control (ISMC) based on Linear Quadratic Regulator with Integral action (LQI) as sliding surface for a Vertical Take-Off and Landing (VTOL) System is presented. The main target is check the robustness of ISMC for several experimental tests under parametric uncertainties and external disturbances. The experimental results are compared against LQI controller. In order to validate the proposed controller, the Integral Square Error (ISE) performance index is used. The controllers were implemented on the QNET VTOL trainer.**

Keywords—ISMC, VTOL system, ISE, Linear quadratic regulator

I. INTRODUCTION

In recent years, many studies have been carried out to study of VTOL systems [1] which is an uncertain system that can be influenced by both matched and mismatched types of uncertainties [2]. The uncertainties could affect the system performance or even devastate the system stability, for this reason, researchers are motivated to find out robust control designs for underactuated systems with uncertainties [3]. For controlling VTOL systems, robust and adaptive control are proposed, but there is a big difference between these controllers, robust control assures that if the changes are within given limits there is no need to change the control law, while adaptive control is mainly focused with control law changing itself [4]. Sliding mode control (SMC) is one of the most effective and efficient control algorithm in dealing with a large kind of uncertain systems [5], for example, motor control, robotic control and flight control [6], but the main SMC problem is the chattering which is an undesired phenomenon [2]. Integral Sliding Mode (ISMC) is similar to SMC because it is insensitive to external disturbance and parameters uncertainty [7]. ISMC is better for the control of an underactuated system because it supplies an extra degree of freedom in control [8]. This controller can be easily incorporated with other robust control methods, such as linear matrix inequality (LMI), and linear quadratic regulator (LQR) to treat with the unmatched uncertainties [3]. In this study, LQI control is considered since its technique involves optimization of a cost function in which the state variables are weighted according to their influence in the control action to seek appropriate performance of the controller [9].

In this paper, an ISMC is proposed for control of VTOL System and a LQI sliding surface is defined. The effectiveness of the design control law was evaluated using the QNET VTOL trainer. To illustrate the effectiveness of the ISMC, three different tests will be considered. The tests were: Step change reference, uncertain physical parameter and external Disturbance Test. In each test, both controllers were compared to check the robustness in terms of integral square error (ISE) index. The brief outline of this paper is as follows: In Section II, the system modelling is introduced. In Section III, the controller design is detailed. Experimental results are provided in Section IV. Finally, Section V contains the conclusion.

II. SYSTEM MODELLING

The QNET VTOL trainer is a one degree-of-freedom (1 DOF) helicopter. The system consists of a variable speed fan, mounted on the end of an arm. The fan and arm assembly pivot about an axis attached to an encoder, when a positive voltage is applied to the DC motor, a lift force is generated causing a lifting of the propulsion system [10]. In this study the model from the manufacturer's manual is used [11]. The components of QNET VTOL Trainer are labeled in Fig.1 and are described in Table I.

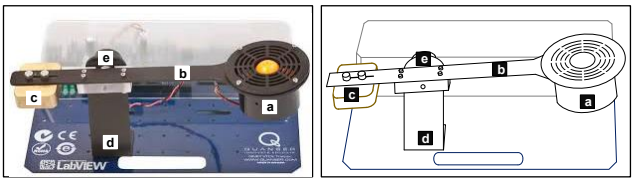

Fig. 1. Vertical Take-off landing QNET VTOL Trainer [11].

TABLE I. QNET VTOL SYSTEM COMPONENTS

ID	Description
a	DC Motor
b	VTOL body
c	Counterweight
d	Support arm
e	Encoder

It is necessary to divide into two subsystems to reduce the complexity of VTOL dynamics:

- The fan motor dynamics
- Flight dynamics

978-1-5386-7612-7/18/$31.00 ©2018 IEEE
DOI 10.1109/INCISCOS.2018.00012

This allows the design of the controllers for two loop control. Fig. 2 illustrates two loop control structure for QNET VTOL.

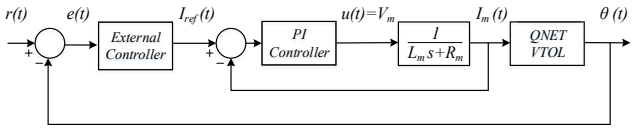

Fig. 2. Control structure scheme for QNET VTOL system.

PI controller controls the motor current around a current reference $I_{ref}(t)$ and an external controller regulates pitch angle $\theta(t)$ around an angle of reference $r(t)$. The transfer function of motor dynamics is described as:

$$I_m(s) = \frac{V_m(s)}{R_m + L_m s} \tag{1}$$

where $V_m(s)$ is the input voltage of motor and $I_m(s)$ is the output current of motor. The pitch angle with respect to current of QNET VTOL system is defined as follows:

$$J\ddot{\theta} + B\dot{\theta} + K\theta = k_t I_m \tag{2}$$

To find the transfer function of pitch angle equation, it is necessary to take the Laplace Transform of (2).

$$\frac{\theta(s)}{I_m(s)} = \frac{K_t}{Js^2 + Bs + K} \tag{3}$$

By converting from transfer function (3) to a state space representation. The dynamic model has the following form:

$$\dot{x}(t) = Ax(t) + Bu(t) \tag{4}$$

$$y(t) = Cx(t)$$

we choose the state vector $\boldsymbol{x} = [\theta \quad \dot{\theta}]^T = [x_1 \quad x_2]^T$, the input $u = I_m$ and the output $x_1 = \theta$. The state space QNET VTOL model is showed as follows:

$$\dot{x}(t) = \begin{bmatrix} 0 & 1 \\ -\frac{K}{J} & -\frac{B}{J} \end{bmatrix} x(t) + \begin{bmatrix} 0 \\ \frac{k_t}{J} \end{bmatrix} u(t) \tag{5}$$

$$y(t) = [1 \quad 0]x(t)$$

The QNET VTOL system parameters are presented in Table II.

By substituting the values of Table II, the state space model is obtained as:

$$A = \begin{bmatrix} 0 & 1 \\ -10.749 & -0.576 \end{bmatrix}, B = \begin{bmatrix} 0 \\ 3.112 \end{bmatrix}, C = [1 \quad 0] \tag{6}$$

By analyzing QNET VTOL system in (6), the pair (A, B) is controllable and the pair (A, C) is observable.

TABLE II. QNET VTOL SYSTEM PARAMETERS

Description	Parameter	Unit
Stiffness	$K = 0.0373$	Nm/rad
Viscous friction constant	$B = 0.002$	Nms/rad
Moment of inertia acting about the pitch axis	$J = 0.00347$	kgm^2
Torque constant	$k_t = 0.0108$	Nm/A
DC Motor resistante	$R_m = 3$	Ω
DC Motor Inductance	$L_m = 0.0583$	H
Proportional contant PI controller	k_p=0.25	
Integral contant PI controller	$k_i = 100$	

III. CONTROLLER DESING

In this section, two controllers are designed for QNET VTOL. LQI controller and ISMC are introduced for system to achieve the set-point in different proposed tests.

A. LQI Controller

LQI controller allows the system to hold the pitch angle of QNET VTOL at desired value [8]. In order to reduce the steady-state error, integral of the error ε is added to the state feedback control as shown in Fig. 3.

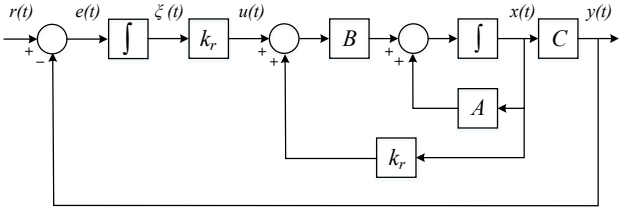

Fig. 3. LQI control scheme for QNET VTOL system.

where $K_r = [k_1 \quad k_2]$ is the vector used for the feedback control law and k_i is the integral error parameter. The tracking error is defined as:

$$e(t) = r(t) - Cx(t) \tag{7}$$

however, the error can be expressed as:

$$e(t) = \dot{\varepsilon}(t) \tag{8}$$

by introducing ε as new state to the system, an extended system can be written as:

$$\begin{bmatrix}\dot{x}(t)\\ \dot{\varepsilon}(t)\end{bmatrix} = \begin{bmatrix}A & 0\\ -C & 0\end{bmatrix}\begin{bmatrix}x(t)\\ \varepsilon(t)\end{bmatrix} + \begin{bmatrix}B\\ 0\end{bmatrix}u(t) + \begin{bmatrix}0\\ 1\end{bmatrix}r(t) \tag{9}$$

Now, the extended system will be named as follows:

$$x_v(t) = \begin{bmatrix}x(t)\\ \varepsilon(t)\end{bmatrix}, A_v = \begin{bmatrix}A & 0\\ -C & 0\end{bmatrix}, B_v = \begin{bmatrix}B\\ 0\end{bmatrix} \tag{10}$$

The LQR method is used minimizes the performance index and can be expressed as:

$$J = \int_0^\infty [x_v^T(t)Qx_v(t) + u^T(t)Ru(t)]dt \tag{11}$$

where $(Q \geq 0)$ is a symmetric and positive semidefinite matrix which penalizes the states and $(R > 0)$ is a symmetric and positive definite matrix which penalizes the input. The algebraic Riccati equation is defined as:

$$PA_v + A_v^T P - PB_v R^{-1} B_v^T P + Q = 0 \tag{12}$$

where P is solution of (12). The state-feedback optimal gains are determined by:

$$K_{lqi} = R^{-1}B_v^T P \tag{13}$$

The feedback control law is defined as:

$$u(t) = -K_{lqi}x_v(t) \tag{14}$$

where $K_{lqi} = [K \quad k_i]$ is the state-feedback gains vector. The cost function depends of Q and R matrices and for this purpose are expressed as:

$$Q = \begin{bmatrix}q_1 & 0 & 0\\ 0 & q_2 & 0\\ 0 & 0 & q_3\end{bmatrix}, \qquad R = [\varphi] \tag{15}$$

The parameters q_1, q_2, q_3 and φ were selected as the inverse of the square of error for $\boldsymbol{x} = [\theta \quad \dot{\theta}]^T$ and $u(t)$ [12] [13] in order to achieve the best response of pitch angle.

B. Integral-Optimal Sliding Mode Controller Design

This subsection shows the design of ISMC with a LQI surface for QNET VTOL system because this controller guaranteed which the error and its derivatives reach zero value [7]. The proposed control scheme of QNET VTOL trainer is illustrated in Fig. 4.

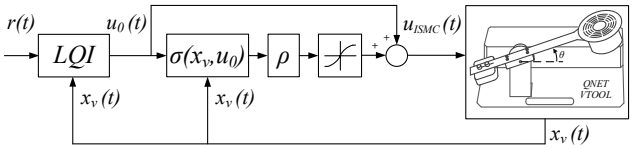

Fig. 4. ISMC control scheme for QNET VTOL system.

This controller has two components: a continuous $u_c(t)$ and discontinuous $u_d(t)$.

$$u_{ISMC}(t) = u_c(t) + u_d(t) \tag{16}$$

In order to apply the ISMC, the first step is to choose a sliding surface [14], in this case the surface is considered as:

$$\sigma(t) = Gx_v(t) - Gx_v(0) - G\int_0^t \left(A_v x_v(\tau) + B_v u_0(\tau)\right) d\tau \tag{17}$$

where $G \in \mathbb{R}^{mxn}$ is a design matrix. In this paper G is selected as follows [15]:

$$G = (B_v^T B_v)^{-1} B_v^T \tag{18}$$

$u_0(t)$ is a nominal controller which can be designed using any feedback approach. $u_0(t)$ is selected as:

$$u_0(t) = -K_{lqi}x_v(t) \tag{19}$$

The continuous part of the controller $u_c(t)$ is provided with the condition to keep the output on the sliding surface $\dot{\sigma}(t) = 0$. By replacing $\dot{x_v}(t)$ in (10), we get the following:

$$\dot{\sigma}(t) = G\dot{x_v}(t) - G[Ax_v(t) + B_v u_0(t)] = 0 \tag{20}$$

and substituting $\dot{x_v}(t) = A_v x_v(t) + B_v u(t)$ in (20), we have:

$$\dot{\sigma}(t) = G[A_v x_v(t) + B_v u(t)] - G[A_v x_v(t) + B_v u_0(t)] = 0 \tag{21}$$

By resolving (20) and considering $u(t) = u_{eq}(t)$, the continuos part of the controller $u_c(t)$ is obtained as:

$$u_c(t) = u_0(t) \tag{22}$$

By completing the ISMC control law, the discontinuous component $u_d(t)$ is added:

$$u_d(t) = -\rho(GB)^{-1} sign\big(\sigma(t)\big) \tag{23}$$

Control law for ISMC is obtained by replacing (19) and (23) in (16):

$$u_{ISMC}(t) = -K_{lqi}x_v(t) - \rho(GB)^{-1} sign\big(\sigma(t)\big) \tag{24}$$

The reachability condition must be satisfied as follows:

$$\sigma(t)\dot{\sigma}(t) < 0 \tag{25}$$

By substituting (21) and (24) into (25), we obtained:

$$-\rho\, sign\big(\sigma(t)\big)\, \sigma(t) < 0 \tag{26}$$

Therefore, by analyzing:

$$if\ \sigma(t) > 0\ \rightarrow sign(\sigma(t)) > 0 \tag{27}$$

$$if\ \sigma(t) < 0\ \rightarrow sign(\sigma(t)) < 0$$

The constant ρ must be positive to satisfy (26). Finally, to reduce the chattering effect [14], $u_d(t)$ can be rewritten as a sigmoid function:

$$u_d(t) = -\rho(GB_v)^{-1} \frac{\sigma(t)}{|\sigma(t)| + \delta} \tag{28}$$

where δ is a chattering parameter reduction. The proposed control law with reduction of chattering effect is described as follows:

$$u_{ISMC}(t) = -K_{lqi}x_v(t) - \rho(GB_v)^{-1} \frac{\sigma(t)}{|\sigma(t)| + \delta} \tag{29}$$

IV. Experimental Results

In this section, the experimental tests are presented. The controllers were implemented in the QNET VTOL trainer which is compatible with LabVIEW 2017 software. The tests were run a computer with an Intel(R)Core(TM) i7-5500U CPU @ 2.40GHz. The developed program for controlling QNET VTOL use the ODE solver method Runge - Kutta1 (Euler).

The tests are:

- Step change reference
- Uncertain physical parameter
- External disturbance

Matrices Q and R were selected by trial and error until achieving the lowest ISE index.

$$Q = \begin{bmatrix} 91.19 & 0 & 0 \\ 0 & 0 & 0 \\ 0 & 0 & 91.19 \end{bmatrix}, \qquad R = [1] \tag{30}$$

By solving (12) with LQR Matlab function, the feedback gain K_{lqi} was obtained and G was calculated into (18). In the same way, the values of δ, ρ were selected by trial and error until achieving the lowest ISE index and these are showed in Table III.

TABLE III. Tunnig Parameters For The Proposed Controllers

Parameter	Value
δ	0.505
ρ	1.2
K_{lqi}	$[-8.73 \quad -2.19 \quad 9.55]$
G	$[0 \quad 0.3213 \quad 0]$

The ISE index was used to compare the robustness of the proposed controllers in each test and is given by:

$$ISE = \int_0^t e^2(\tau)d\tau \tag{27}$$

where $e(\tau)$ represents the error between θ_d and θ.

A. Step Change Reference Test

In this test, the change reference is a step from $\theta = 0\ [deg]$ to $\theta_d = 30\ [deg]$ for both controllers as is illustrated in Fig. 5.

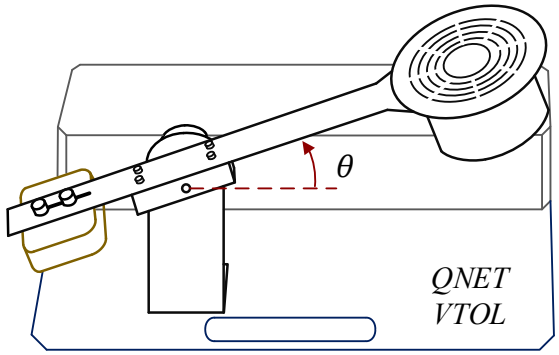

Fig. 5. Step change reference test for QNET VTOL system.

In Fig. 6a. LQI controller and in Fig. 7a ISMC controller show that the system reaches a desired angle for a step change reference tests. The control actions of both controllers are within the permitted ranges by the manufacturer, these signals are

shown in Fig. 6b for LQI controller and in Fig. 7b for ISMC controller.

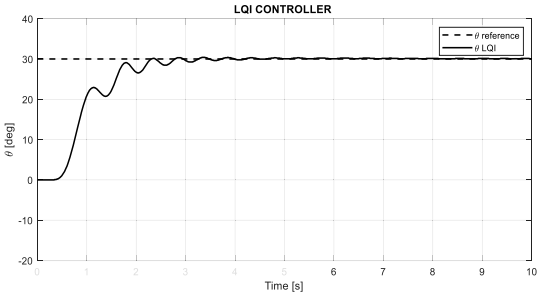

a) Step response of QNET VTOL System.

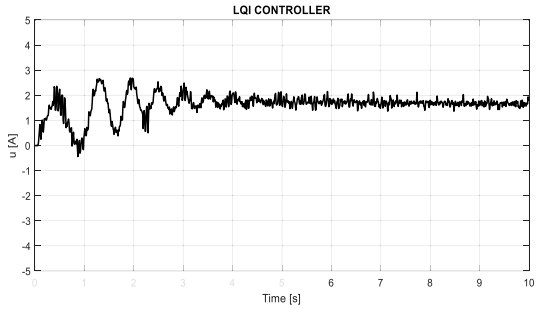

b) Control action.

Fig. 6. Experimental results of LQI controller for a step change reference.

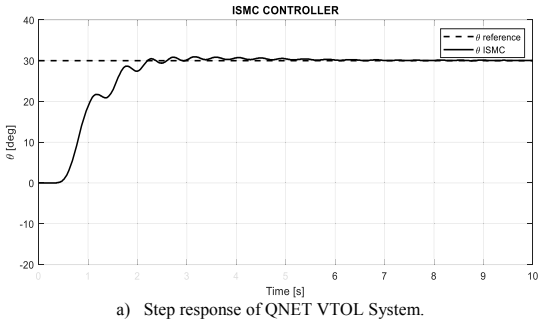

a) Step response of QNET VTOL System.

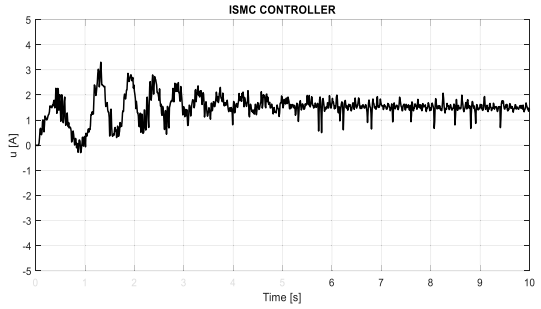

b) Control action.

Fig. 7. Experimental results of ISMC controller for a step change reference.

B. Uncertain Physical Parameter Test

The system was altered adding a small iron mass on QNET VTOL body. This uncertain object has a mass of $m = 0.25\ [Kg]$ which is located $D = 0.085\ [m]$ from pivot point as is showed in Fig. 8. The objective of this test is to verify if the controllers reach the desired angle without problems.

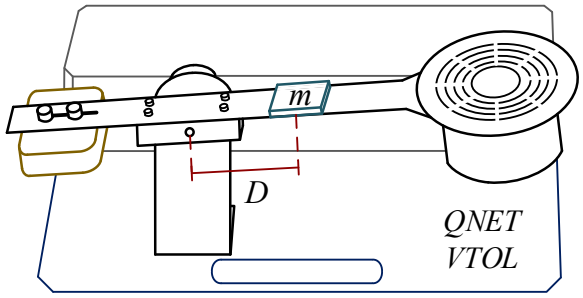

Fig. 8. Uncertain in physical parameter test for QNET VTOL system.

In Fig. 9 and Fig. 10, the controller's performance and the corresponding control signal respectively are presented. One can notice, the overshoot of ISMC controller is lower than LQI controller. Despite having more weight on the QNET VTOL body, the control actions of both controllers are within the range. Allowed range : $\pm 3\ [A]$. Fig. 9b and Fig.10b present control actions for the uncertain physical parameter test.

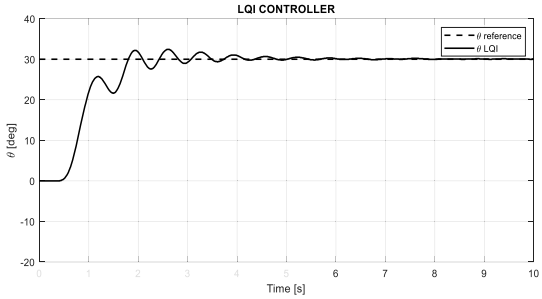

a) Step response of QNET VTOL System.

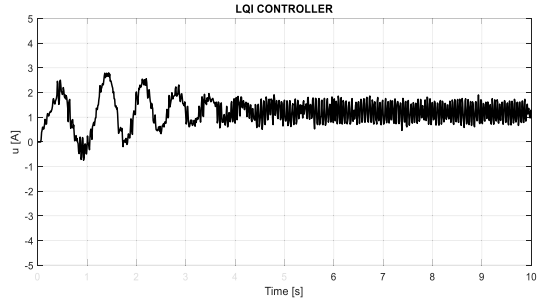

b) Control action.

Fig. 9. Experimental results of LQI controller for an uncertain parameter.

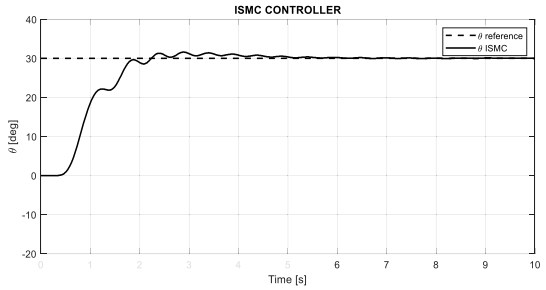

a) Step response of QNET VTOL System.

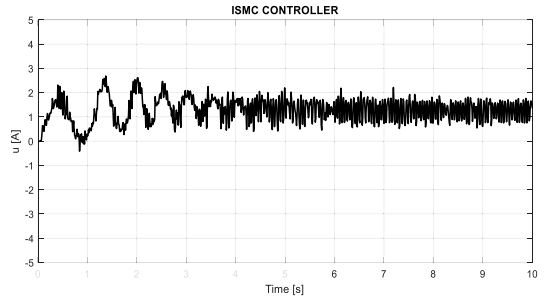

b) Control action.

Fig. 10. Experimental results of ISMC controller for an uncertain parameter.

C. *External Disturbance Test*

In this test, the QNET VTOL system must maintain an $\theta_d = 0\ [deg]$ when a ball ($m_b = 0.05[Kg]$) falls from an altitude of $L = 0.05[m]$ as is illustrated in Fig. 11.

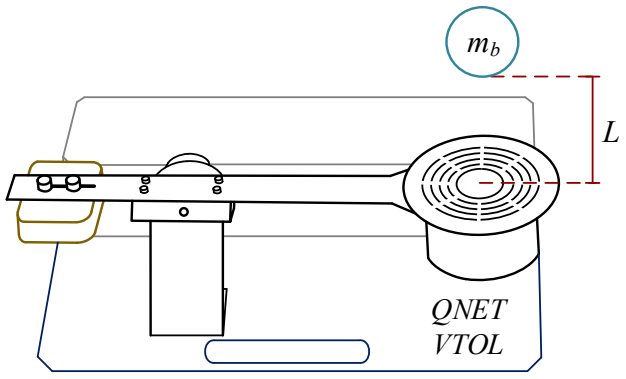

Fig. 11. External Disturbance Test for QNET VTOL system.

In Fig. 12a shows the tracking performance of LQI controller. It can be seen that the response this controller settles at origin value after approximately 15 seconds, while in Fig. 13a, ISMC controller settles at origin after approximately 8 seconds.

In this case, the control action of ISMC controller showed in Fig. 13b is stronger than LQI controller. In this way, the QNET VTOL system settles at the origin faster.

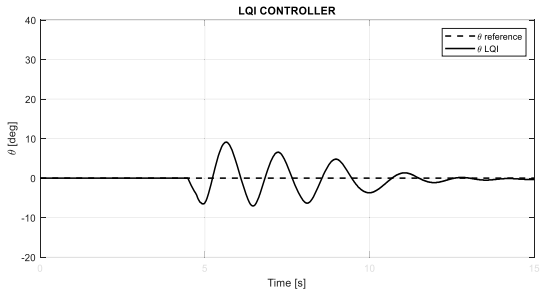

a) QNET VTOL System response.

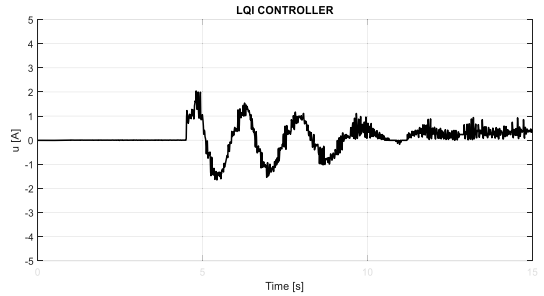

b) Control action.

Fig. 12. Experimental results of LQI controller for an external disturbance.

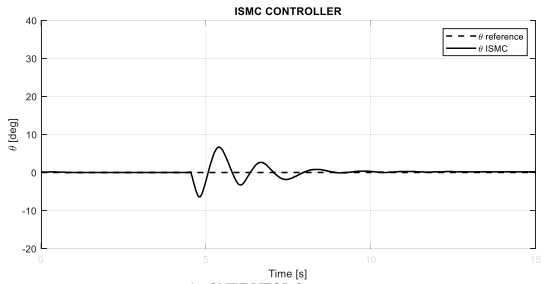

a) QNET VTOL System response.

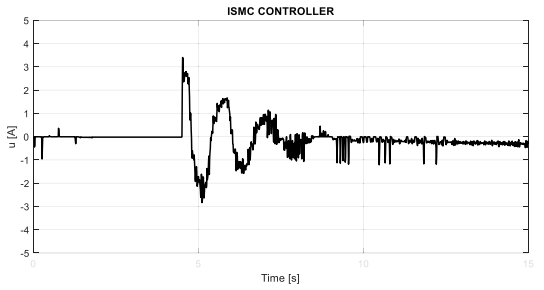

b) Control action.

Fig. 13. Experimental results of ISMC controller for an external disturbance.

In Table IV presents the comparison between both controllers in each test carried out. In the step change

reference test and the uncertain physical parameter test, both controllers have a minimum variation between them because of the good performance and excellent robustness. On the other hand, in the external disturbance test, LQI controller produces the unsatisfactory performance and not robust with respect to disturbances.

TABLE IV. ISE COMPARISON

ISE Step change reference test			
Var.	**ISE LQI**	**ISE ISMC**	**% Δ**
θ	7.328	7.040	4.01
Uncertain Physical Parameter Test			
Var.	**ISE LQI**	**ISE ISMC**	**% Δ**
θ	7.292	7.087	2.85
External Disturbance Test			
Var.	**ISE LQI**	**ISE ISMC**	**% Δ**
θ	12.000	3.240	114.96

ACKNOWLEDGMENT

CONCLUSIONS

In this article, ISMC and LQI controller based on model are successfully designed and implemented on the QNET VTOL trainer. ISMC controller present lower ISE index than LQI controller for all tests. The robustness of the proposed controller was evident for external disturbance test when ISMC controller settles at reference after approximately 8 seconds while LQI controller settles at reference value after 15 seconds. The most significant betterment of using ISMC is the reducing of the settling time response of QNET VTOL system.

REFERENCES

[1] G. Haisheng y L. Jinkun, «Sliding Mode Control for VTOL Aircraft Based on High-Gain Observer», en *Instrumentation, Measurement, Computer, Communication and Control (IMCCC), 2012 Second International Conference on*, 2012, pp. 305–309.

[2] S. Mondal y C. Mahanta, «Observer based sliding mode control strategy for vertical take-off and landing (VTOL) aircraft system», en *Industrial Electronics and Applications (ICIEA), 2013 8th IEEE Conference on*, 2013, pp. 1–6.

[3] J.-X. Xu, Z.-Q. Guo, y T. H. Lee, «Design and implementation of integral sliding-mode control on an underactuated two-wheeled mobile robot», *IEEE Trans. Ind. Electron.*, vol. 61, n.º 7, pp. 3671–3681, 2014.

[4] D. Y. Dube y R. K. Munje, «Modeling and control of Unmanned Aerial Vehicle», en *2015 International Conference on Energy Systems and Applications*, 2015, pp. 641-644.

[5] S. Sanjari y S. Ozgoli, «Generalized Integral Siding Mode Manifold Design: A Sum of Squares Approach», *ArXiv Prepr. ArXiv150308642*, 2015.

[6] K.- Shyu, G.- Lai, y Y.- Tsai, «Optimal position control of synchronous reluctance motor via totally invariant variable structure control», *IEE Proc. - Control Theory Appl.*, vol. 147, n.º 1, pp. 28-36, ene. 2000.

[7] A. K. Hamoudi, «Design an Integral Sliding Mode Controller for a Nonlinear System», *Al-Khwarizmi Eng. J.*, vol. 13, n.º 1, pp. 138–147, 2017.

[8] B. Shilpa, V. Indu, y S. R. Rajasree, «Design of an underactuated self balancing robot using linear quadratic regulator and integral sliding mode controller», en *2017 International Conference on Circuit ,Power and Computing Technologies (ICCPCT)*, 2017, pp. 1-6.

[9] K. Singh y A. Singh, «Design and analysis of LQR based controller for reactive power compensation», en *2016 IEEE 6th International Conference on Power Systems (ICPS)*, 2016, pp. 1-5.

[10] R. L. Pereira y K. H. Kienitz, «Experimental investigation of nonlinear controllers applied to a 3DOF hover: SMC via ALQR approach», en *2015 23rd Mediterranean Conference on Control and Automation (MED)*, 2015, pp. 520-524.

[11] QUANSER, «QNET VTOL User Manual», vol. 1, p. 27, 2011.

[12] R. Murray, *Optimization Based-control (California Institute of Technology)*. 2009.

[13] M. Herrera, «A Blended Sliding Mode Control with Linear Quadratic Integral Control based on Reduced Order Model for a VTOL System.», 2017.

[14] O. Camacho y C. A. Smith, «Sliding mode control: an approach to regulate nonlinear chemical processes», *ISA Trans.*, vol. 39, n.º 2, pp. 205-218, abr. 2000.

[15] M. T. Hamayun, C. Edwards, y H. Alwi, *Fault Tolerant Control Schemes Using Integral Sliding Modes*. Springer International Publishing, 2016.